Journal of Materials and Environmental Science
ISSN : 2028-2508
e-ISSN : 2737-890X
CODEN : JMESCN

J. Mater. Environ. Sci., 2025, Volume 16, Issue 12, Page 2186-2206

http://www.jmaterenvironsci.com

Effect of kenaf fibers on engineering and durability properties of alkali-activated compressed earth bricks (CEB) using a NaOH solution

Seick Omar SORE [1,2] *, Philbert NSHIMIYIMANA [2], Diatto Kevin NAMOULNIARA [1], Souleymane OUEDRAOGO [2], Kader BANAOU DJIBO [2], Mamounata SEMDE [3], Abdoulaye SANA [4], Adamah MESSAN [2]**

[1]*Département Génie Civil de l'Institut Universitaire de Technologie / Laboratoire de Chimie et Energies Renouvelables (LaCER), Unité de Recherche en Physico Chimie et Technologie des Matériaux, Université Nazi BONI, B.P.1091 Bobo 01, Burkina Faso*

[2] *Laboratoire Eco-Matériaux et Habitats Durables (LEMHaD), Institut International d'Ingénierie de l'Eau et de l'Environnement (Institut 2iE), Rue de la Science, 01, BP 594 Ouagadougou 01, Burkina Faso*

[3] *Programme Alimentaire Mondial, B.P 575 Ouagadougou, Burkina Faso*

[4] *Direction Régionale de l'Agriculture des Ressources Animales et Halieutiques du Nord, Ouahigouya, Burkina Faso*

**Corresponding author, Email address: seickomar9@yahoo.fr*
***Corresponding author, Email address: philbert.nshimiyimana@2ie-edu.org*

Received *19 Aug 2025,*
Revised *25 Oct 2025,*
Accepted *26 Oct 2025*

Keywords:
- ✓ *Lateritic material;*
- ✓ *Compressed earth blocks*
- ✓ *Alkali-activation;*
- ✓ *Kenaf fibers;*
- ✓ *Engineering properties*

Citation*: Sore S.O., Nshimiyimana P., Namoulniara D. K., Ouedraogo S., Banaou Djibo K., Semde M., Sana A., Messan A. (2025) Effect of kenaf fibers on engineering and durability properties of alkali-activated compressed earth bricks (CEB) using a NaOH solution, J. Mater. Environ. Sci., 16(12), 2186-2206*

Abstract: This study aims to evaluate the physico-mechanical, thermal and durability, properties of compressed earth bricks (CEBs) activated with an alkaline solution and reinforced with kenaf fibres. The CEBs (29.5 × 14 × 9 cm³) were made from lateritic soil and activated with a 12M NaOH solution, dosed at 20% of the soil mass. Different mass fractions of kenaf fibres (0%, 0.5%, 1%, and 1.5%) were incorporated to study their influence. After a 45-day curing, including 7 days under the laboratory conditions (30 ± 5 °C) and 14 days of under ambient conditions under black polyane film (40 ± 5°C), followed by 24 days of sun drying, the CEBs underwent physical, mechanical, thermal and durability characterisations. The results indicate an overall decrease in physico-mechanical properties with increasing fibre content, except for flexural strength. The latter reached an optimum at 1% fibre content, with a value of 1.49 MPa. Although compressive strengths decreased, they remained compatible with the requirements of earthen construction. However, the addition of fibre had a beneficial effect on the thermal properties. The CEB with 1.5% fibres exhibited the best thermal performance, with a thermal conductivity of 0.48 W/m·K and a diffusivity of 0.24 mm²/s, values close to those of unstabilized CEBs (0.43 W/m·K and 0.22 mm²/s, respectively). Durability indicators also decreased, but remained acceptable, for non-erodible, non-absorbent, and abrasion-resistant CEB.

1. Introduction

Population growth and increasing urbanization, particularly in Africa, are driving a rising demand for construction materials to meet the needs of an expanding population. However, in the face of climate challenges and greenhouse gas emissions, it is imperative to develop more sustainable construction solutions. Among traditional materials, earth holds a central place in construction history and is used in various forms, such as rammed earth (Giuffrida *et al.,* 2019), cob (Hamard *et al.,* 2016) or adobe (Sanou, Ouedraogo, *et al.,* 2024). In Africa, more than two-thirds of the population lives in

earthen dwellings (Bobet et al., 2020). Compressed Earth Bricks (CEB), an improved version of the adobe, are now widely used in diverse architectural projects worldwide (Kagonbé *et al.,* 2023). However, without stabilization, these blocks exhibit increased sensitivity to water, leading to rapid degradation due to weathering. To enhance their mechanical performance and durability, chemical stabilization is necessary. Initial research primarily focused on conventional binders, such as Portland cement (Latha *et al.,* 2023) or lime (Dime et al. 2022; Nshimiyimana *et al.,* 2020). However, these materials, in addition to being costly, have significant environmental impacts (Labiad *et al.,* 2022). These limitations have motivated the search for eco-friendly and economical alternatives. In this context, recent studies have focused on geopolymer binders obtained through the alkaline activation of aluminosilicate precursors such as metakaolin, fly ash, and silica fume (Idriss *et al.,* 2022; Ongpeng *et al., 2020; Sore et al., 2018)*. Among these aluminosilicate sources, metakaolin is one of the most widely used. However, it is produced by calcining kaolinite clay at temperatures between 600 and 800°C (Kostas *et al.,* 2007; Ainane *et al.,* 2021), which is an energy-intensive process, particularly in developing countries.

To further reduce the carbon footprint, researchers have experimented with the direct alkaline activation of laterite or clay, major components of compressed earth bricks (CEBs), using sodium hydroxide (NaOH) or silicate (Na_2SiO_3) solutions (Diop *et al.,* 2011; Lemougna *et al.,* 2014; Ramanandraibe *et al.* 2023; El Miz, *et al.* 2024; Sore, *et al.* 2025). These studies demonstrated a significant improvement in mechanical properties and water resistance, with compressive strengths reaching 4.3 MPa (Sore et al. 2025) and remarkable stability after prolonged immersion. At the same time, the integration of natural fibers into composite materials has garnered growing interest, particularly because of their low cost, biodegradability, and contribution to reducing the carbon footprint (Shinoj *et al.,* 2010; Zak et al. 2016). Tests on fiber-reinforced CEBs using date palm fibers (Taallah & Guettala, 2016), hemp (Zak *et al.,* 2016), sisal (Labiad *et al.,* 2022), coconut (Ghavami *et al.,* 1999), rice straw (Labintan *et al.,* 2019) or kénaf (Sanou, Bamogo, *et al.,* 2024; Serebe *et al.,* 2024) revealed improvements in thermal properties and flexural strength. However, the effects on compressive strength remain mixed; some authors observed a decrease (Taallah & Guettala, 2016; Zardari *et al.,* 2020), while others reported an increase up to an optimal ratio (0.4% by weight for kenaf (Serebe *et al.,* 2024); 25% by volume for rice straw (Labintan *et al.*, 2019).

Burkina Faso contains significant clay resources, including kaolinite minerals, which are particularly suitable for geopolymerization (Ghayti *et al.*, 2021; Konstantinos Komnitsas *et al.* 2021; Sore *et al.*, 2025). Additionally, the country generates a substantial amount of agricultural residues, such as rice husks, kenaf fibers, and peanut shells, offering promising opportunities for the valorisation of local materials in the construction sector. In this context, this study aims to analyze the effect of incorporating kenaf fibers (at contents ranging from 0 to 1.5%) on the physico-mechanical, thermal and durability properties of alkali-activated compressed earth bricks (CEBs) using a 12M NaOH solution (20%), compared to non-stabilized CEBs. The results will help to assess the potential of this innovative approach for more sustainable, economically viable, and environmentally friendly construction.

2. Materials and methods

2.1 Materials: Aluminosilicate and activator

The aluminosilicate used was the 0/5 mm fraction of lateritic soil (**Figure 1)** extracted from the Kamboinse quarry (12°29’24″’’N, 1°33’07’’″ W, altitude 317 m). The physical and geotechnical characteristics of the studied soils are presented in **Table 1**. The fine fraction content (particles smaller

than 80 µm) was approximately 78.12%. This high-fine fraction acted as a filler in the formulation of compressed earth bricks (CEB). It has a methylene blue value of 0.85 g/100 g and a plasticity index (Ip) of 25.9%. These characteristics, combined with the percentages passing through the 80 µm and 2 mm sieves, allowed it to be identified as a B6-class soil, meeting the acceptability criteria for earth brick production (Houben & OA, 1998). Furthermore, according to the Casagrande plasticity chart, this soil is classified as inorganic clay of high plasticity (CH), confirming its suitability for the production of compressed earth blocks (CEB). This classification is illustrated in **Figure 2**.

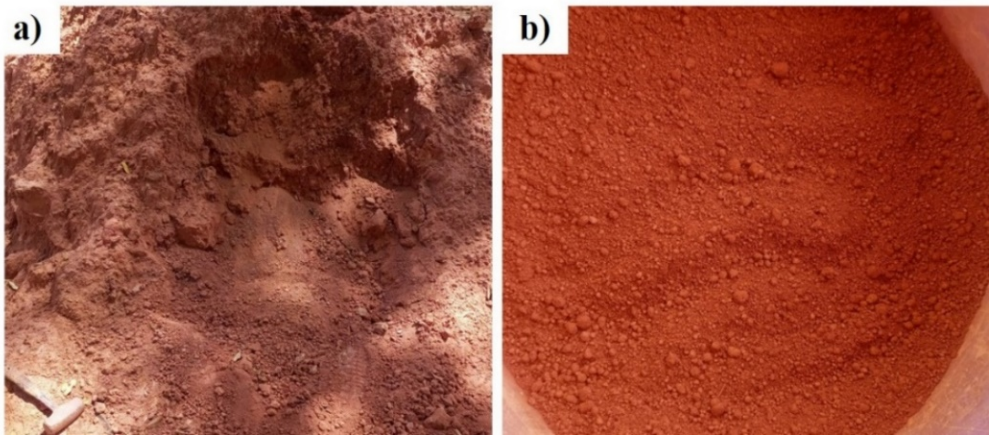

Figure 1. Lateritic soil at the sampling site (**a**) and after sieving to 5 mm (**b**)

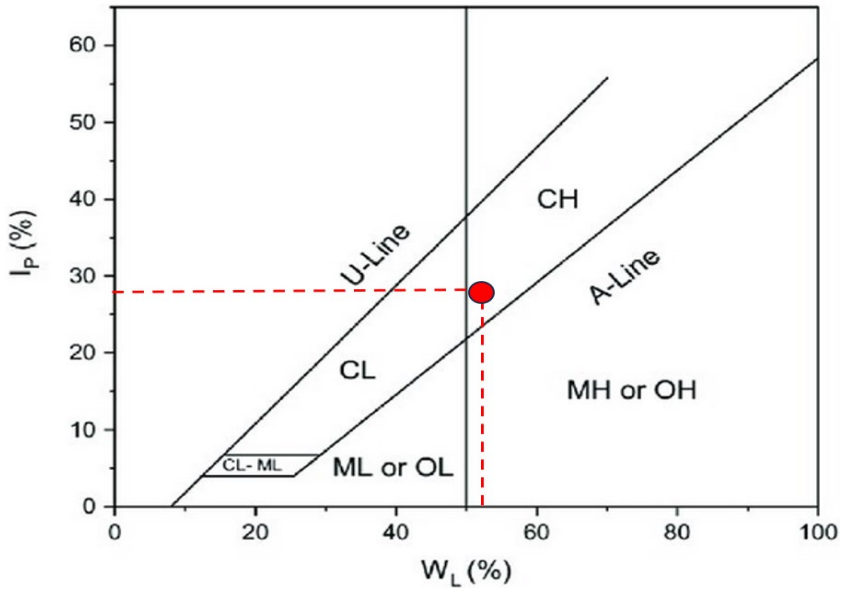

Figure 2. Soil classification according to the Casagrande diagram)

The chemical composition, as determined by inductively coupled plasma atomic emission spectroscopy (ICP-AES) (**Table 2**), showed that the sample consisted mainly of silica (55.3%) and alumina (28.2%) with a relatively low iron oxide content (9.05%), which is likely responsible for its reddish color. Mineralogical characterization by XRD (**Figure 3**), combined with the chemical composition, allowed the estimation of the mineral phases as 63.10% kaolinite, 18.4% goethite, and 16.8% quartz. These chemical and mineralogical characteristics confirm that the laterite used can be considered an aluminosilicate with a high kaolinite content that is conducive to a geopolymerization reaction in the presence of an alkaline solution (Sore *et al.*, 2025).

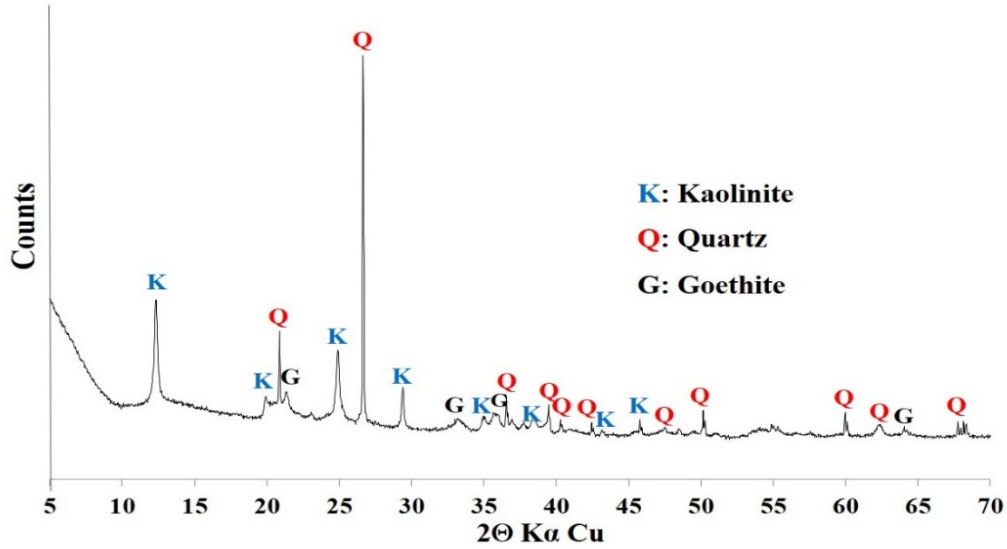

Figure 3. X-ray diffraction pattern of the lateritic soil

Figure 4. Loose kenaf fibres (**a**) after cutting (**b**) into 3 cm (**c**)

Table 1. Physical characteristics of lateritic soil

Particle size analysis (AFNOR NF EN 933-1, 2012; AFNOR NF ISO 17892-4, 2018)	Corse sand [2 – 5 mm] (%)	5.72
	Medium sand [0.63 –2 mm] (%)	10.28
	Fine sand [80 µm – 0.63 mm] (%)	5.88
	Silt [2µm – 80 µm] (%)	48.12
	Clayey fraction < 2 µm (%)	30
Atterberg limits)AFNOR NF EN ISO 17892 -12/A1, 2021(	Liquid limit (%)	53.3
	Plastic limit (%)	27.4
	Plasticity index - IP (%)	25.9
Absolute density by pycnometer (g/cm^3)		2.88
Normal Proctor water content (%) (NF P94-03, 2014)		26.03
Methylene blue test (g/100g) (AFNOR NF EN 933-9, 2022)		0.85

Table 2. Chemical and mineralogical composition of lateritic soil

Chemical composition											
Oxides	SiO_2	Al_2O_3	Fe_2O_3	CaO	K_2O	MgO	MnO_2	TiO_2	P_2O_5	Cr_2O_3	LOI
Clay (%)	55.3	28.2	09.05	0.01	0.46	0.16	0.03	0.92	0.06	0.02	5.79
Mineralogical composition											
Crystalline phase	Kaolinite		Goethite		Quartz		Balance				
Percentage (%)	63.10		18.40		16.80		1.70				

Sodium hydroxide (NaOH) was used as the activating solution at a concentration of 12 M, which was prepared by dissolving 480 g of NaOH crystals (99% purity) in 1 L of distilled water. It was usable for 24 h after preparation. A dosage of 20% relative to the mass of laterite was used for all formulations, as it showed highly satisfactory performance according to a previous study conducted by Sore et al. (Sore *et al.,* 2025). The kenaf fibers (**Figure 4)** used were sourced from a site at the Institute of Environment and Research in Agriculture (INERA) located in the village of Farakobâ (11° 6′ 0" North, 4° 19′ 60" West), on the western outskirts of Bobo-Dioulasso. The fibers used in this study were cut to a length of 3 cm (**Figure 4b,c)**. They have already been characterized by Sanou et al. (Sanou, Bamogo, *et al.,* 2024) and Serebe et al. (Serebe *et al.,* 2024), and their properties, presented in **Table 3**, show that they have an average diameter of 10 µm, apparent density of 1.05 g/cm³, and water absorption rate of 307%. They were rich in cellulose (71% by weight), hemicellulose (20% by weight), and lignin (4% by weight). Owing to their high cellulose content and rough surface, kenaf fibers exhibit high tensile strength, estimated at 820 MPa.

Table 3. Characteristics of kenaf fibres (Serebe et al., 2024)

Physical properties	Water absorption capacity (%)	307
	Density (g/cm^3)	1.05
	Diameter (µm)	10
Biochemical composition	Cellulose (%)	71
	Hemicellulose (%)	20
	Lignin (%)	4
Tensile strength (MPa)		820 ± 202

2.2 Experimental methods

2.2.1 CEBs manufacturing process

This study aims to evaluate the effect of incorporating kenaf fibers on the physico-mechanical, durability, and thermal properties of alkali-activated compressed earth blocks (CEBs). To this, five (05) CEB formulations were developed.

- a reference CEB (CN0K0), without alkali activation or kenaf fiber addition;
- Four CEBs were activated by an alkaline NaOH solution (12M), dosed at 20% of the lateritic soil mass, and reinforced with 3 cm kenaf fibers at varying mass contents (0%, 0.5%, 1%, and 1.5%).

The choice of 20% alkaline dosage was based on a previous study (Sore, Nshimiyimana, Ouedraogo, et al., 2025), which demonstrated that it achieved a compressive strength of 4 MPa, in compliance with the XP P 13-901 standard (XP P13-901, 2017) for earthen construction. **Table 4** lists the detailed compositions of the different tested mixtures.

CEBs are produced by homogeneously mixing laterite and fibers (for fiber-reinforced CEB s), then gradually adding humidification water, followed by NaOH solution. The amount of water **(Eqn. 1)** was determined based on the optimal moisture content of 26.03% (from the standard Proctor test, **Table 1**), adjusted according to the fiber absorption rate (307%), and subtracting the mass of the alkaline solution. The latter was incorporated gradually until the end of mixing, a step that requires a longer time (at least 10 min) depending on the fiber content. The wet mixture was then placed in a mould (29.5 × 14 × 9.5

cm) and compressed at 35 bars using a manual press (TERSTARAM) to form the samples. These were stored in plastic bags for 7 days at ambient temperature (30 ± 5 °C), then covered with a black polyane tarp for a 14-day solar curing period, during which midday temperatures reached 40 ± 5 °C, promoting geopolymerization. After 24 days of sun drying, the CEB s were characterized at the end of 45 days to determine their physico-mechanical, durability, and thermal properties. The manufacturing process is illustrated in **Figure 5:**

$$W_h = \left(W_P \times M_S + T_{af} \times M_F\right) - S_a \qquad \textbf{Eqn. 1}$$

where W_h = CEBs humidification water mass (in grams), W_p = optimal water content of laterite soil (in grams), M_S = mass of dry laterite, T_{af} = Water absorption rate of fibers, M_F = fiber dry mass (in grams), and S_a = mass of alkaline solution (in grams).

Table 4. Mix design of the alkali-activated CEB

Design	CN0K0	CN20K0	CN20K0.5	CN20K1	CN20K1.5
Lateritic soil (g)	7100	7100	7100	7100	7100
NAOH solution 12M(g)	-	1420	1420	1420	1420
Kenaf fibres (g)	-	0	35,5	71	106,5
W_h (g)	1848	428	537	646	755

CNXKY: Compressed earth blocs with X% of N (NaOH solution) and Y% of K (kenaf fibers)

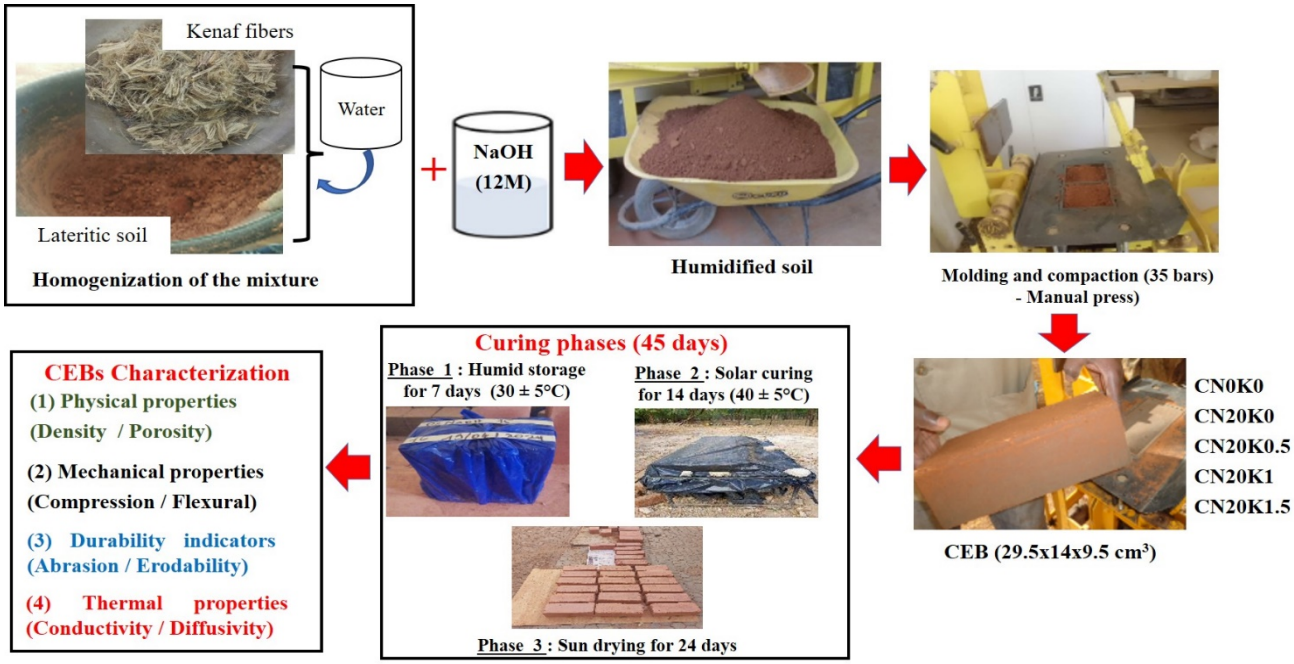

Figure 5. CEBs manufacturing process

2.2.1 Methods for characterising CEBs

This section presents the experimental methods used for the physico-mechanical, durability, and thermal characterization of CEB samples, assessing the impact of alkaline activation and the effect of kenaf fibers on the engineering properties of these construction materials. The majority of these characterizations were performed in accordance with the recommendations of the XP P13-901 standard (XP P13-901, 2017).

- ***Physical properties characterisation methods***

Physical properties, such as apparent density and water porosity of the CEB samples, were determined according to Eqn. (2) and Eqn. (3), respectively:

$$\rho = \frac{M_{dry} \times \rho_W}{(M_{sat.air} - M_{sat.wat})} \times 100 \quad \textbf{Eqn. 2}$$

$$P = \left(\frac{M_{sat.air} - M_{dry}}{M_{sat.air} - M_{sat.wat}}\right) \times 100 \quad \textbf{Eqn. 3}$$

where ρ is the apparent density, ρ_W is the water density, M_{dry} the constant dry mass of the sample (in grams), $M_{sat.air}$ is the saturated mass in air (in grams), $M_{sat.wat}$ the saturated mass in water (in grams), and P is the accessible porosity of the sample under test (%).

The velocity of the propagation of ultrasonic waves through hardened CEBs was measured to assess the compactness of the sample matrix using the Pundit test following the protocol set up by Sore et al. (Sore *et al.,* 2018). Water capillary absorption was determined using the square root of time according to Eqn. 4. The bottom surface of the dried CEBs measuring 29.5×14 cm² was partially immersed in water at a depth of 1 ± 0.5 cm. The wet masses were then measured at intervals corresponding to t = 0.17, 0.5, 1, 2, 4, 8, 16, and 24 h of capillary immersion. The capillary absorption coefficient was calculated using Eqn. 5:

$$WC = \left(\frac{M_{Wt} - M_{dry}}{S}\right) \quad \textbf{Eqn. 4}$$

$$CW_{10min} = 100 \times \left(\frac{M_{W10} - M_{dry}}{S\sqrt{10}}\right) \quad \textbf{Eqn. 5}$$

where WC = Water capillary absorption (g/cm^2. min^{½}), M_{Wt} = wet mass measured at time t (in g), M_{dry} = constant dry mass of the sample (in g), S = sample area (in cm^2), CW_{10min} = capillary absorption coefficient (in g/cm^2. min^{½}).

The reference CEBs (CN0K0) physical properties (density, porosity and water capillary absorption), which contain neither alkaline solution nor kenaf fibers, could not be evaluated due to their susceptibility to water exposure.

- ***Mechanical properties characterisation methods***

The dry and wet compressive strengths were determined using Eqn. 6. The wet compressive strength test was performed on samples of CEBs that had been saturated in water for 2 h.

The three-point flexural strength was determined usingto Eqn. 7. A hydraulic press (ETI-PROETI) with a 300 kN capacity and a loading rate of 0.25 kN/s was used for this purpose. Three samples were tested for each test, and each result displayed was the average of the three samples.

$$R_C = 10 \times \frac{F_r}{S} \quad \textbf{Eqn. 6}$$

$$R_f = 10 \times \frac{1.5 \times F_r L_0}{b \times h^2} \quad \textbf{Eqn. 7}$$

- ***Thermal properties characterisation methods***

The thermal properties (thermal conductivity and diffusivity) of the fiber-reinforced CEBs were measured using a KD2 Pro Thermal Properties Analyzer (Zoma et al., 2020), equipped with an SH-1 dual-needle sensor (length: 30 mm, diameter: 1.3 mm, spacing: 6 mm). This device is based on the transient line heat source method, allowing for the simultaneous measurement of the thermal conductivity and thermal diffusivity after inserting the needles into the tested material.

- ***Durability properties characterisation methods***

The durability indicators assessed in this study were abrasion coefficient and resistance to water erosion (erodibility). To evaluate the abrasion resistance, the surface of the CEB s was subjected to 60 abrasion cycles using a metal brush under a 3 kg load. After the test, the mass losses and abraded surfaces were measured to determine the abrasion coefficient (Ca), as well as the percentage of mass loss attributable to abrasion. The resistance to water erosion was evaluated according to the protocol of Djibo et al. (Djibo *et al.,* 2024), by subjecting a circular surface of 75 mm to a water jet at 500 kPa, a pressure deliberately higher than the 50 kPa recommended by the NZS 1998 standard (Allen *et al.,* 1998) to study the influence of alkaline content and kenaf fibers on erosion resistance under extreme conditions. After testing, the erosion depth was measured using a needle inserted into the sample holes, and the eroded area was quantified relative to the total exposed surface.

3. Results and Discussion

3.1 Physical properties

3.1.1 Apparent density, Porosity accessible to water and Ultrasonic Pulse Velocity

Figure 6 shows the evolution of the apparent density and water-accessible porosity of alkali-activated and kenaf fiber-reinforced compressed earth blocks (CEBs). It was observed that the addition of fibers led to a decrease in the apparent density, while the porosity increased in direct proportion. The estimated optimal variations were -4.11% for density and +9% for porosity. CEBs without an alkaline solution or fibers could not be evaluated for these properties because of their vulnerability upon contact with water. In contrast, the 20% alkali-activated samples without fibers (CN20K0) exhibited the best performance, with a density of 1 659 kg/m³ and a porosity of 34%. Conversely, CEBs containing 1.5% fibers (CN20K1.5) exhibited a lower density (1 591 kg/m³) and higher porosity (37%).

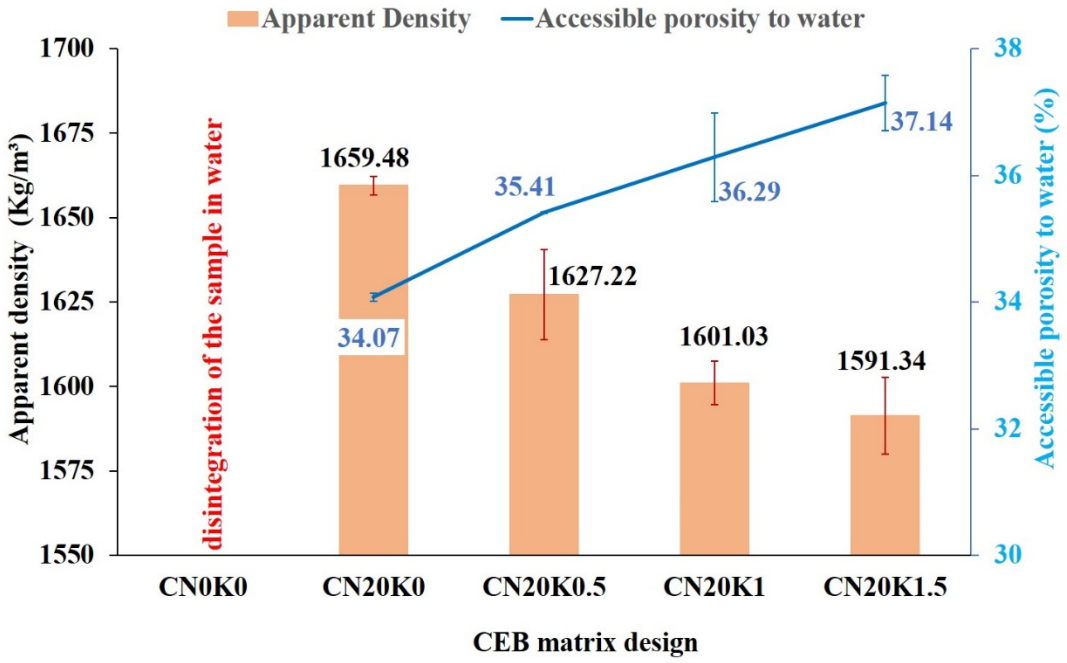

Figure 6. Apparent density and water-accessible porosity of alkali-activated and kenaf-fibers-reinforced CEBs

This reduction in density can be explained by the partial substitution of lateritic soil, which has a high absolute density (2.88), with less dense kenaf fibers (1.05) in a given volume of CEB, as reported by (Taallah & Guettala, 2016; Zak *et al.*, 2016). Furthermore, the increase in porosity with fiber content

may be linked to their hydrophilic nature (**Table 3**). Indeed, incorporating fibers into the lateritic mixture requires additional water during the formulation (**Table 4**). During curing, geopolymerization reactions, accelerated by solar exposure, cause the evaporation of excess water absorbed by the fibers. This phenomenon generates microcavities in the matrix, thereby reducing the density and increasing porosity. Similar results were observed by Labiad et al. (Labiad *et al.*, 2022) on cement-stabilized CEBs reinforced with sisal fibers (0–0.5%). Additionally, Bories et al. (Bories *et al.*, 2015) also reported a decrease in the density of earth bricks with increasing wheat straw content (4 to 8%). The evolution of the compactness of different Compressed Earth Blocks (CEBs), depending on the kenaf fiber content, was evaluated by measuring the ultrasonic pulse velocity (**Figure 7**). This analysis revealed two distinct phases.

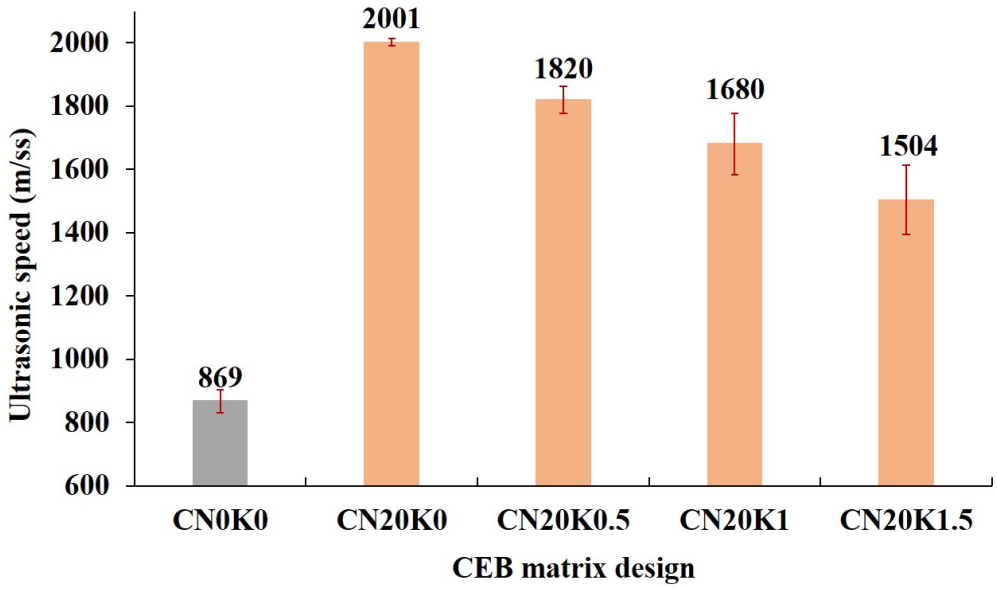

Figure 7. Ultrasonic Pulse Velocity of alkali-activated and kenaf-fibers-reinforced CEBs

First, the ultrasonic velocity was increased from 869 m/s (raw CEB without alkaline solution or fibers, CN0K0) to 2001 m/s (CEB activated with 20% NaOH, CN20K0). This significant increase can be attributed to the reaction of the alkaline solution with kaolinite minerals (Sore, Nshimiyimana, Ouedraogo, *et al.*, 2025), which is the main component of lateritic soil (aluminosilicate source). This reaction leads to the formation of geopolymer gels, which enhance particle cohesion within the matrix, thereby increasing its compactness. A denser structure facilitated the propagation of ultrasonic waves.

Second, the ultrasonic velocity gradually decreased with the incorporation of kenaf fibers, dropping from 2001 m/s (CN20K0) to 1504 m/s for a fiber content of 1.5% (CN20K1.5), representing an optimal reduction of 24.84%. This decline is attributed to the effect of the fibers, which introduce additional porosity into the matrix, thereby slowing wave propagation (Heller-Kallai & Lapides, 2007). These observations are consistent with the bulk density and accessible porosity results (**Figure 6**). Less dense samples with higher porosity exhibited reduced ultrasonic velocity. This is the case, for example, with CEBs of type CN20K1.5 (1591 kg/m³, 37%, and 1504 m/s) compared with CN20K0 (1659 kg/m³, 34%, and 2001 m/s). Similar trends have been reported by Mastali et al. (Mastali *et al.*, 2020) in geopolymer-stabilized fiber-reinforced CEBs (cellulose, basalt, and polypropylene).

3.1.2 Capillary absorption

Figure 8 presents the results of the water absorption coefficient by capillarity (CW_{10}) of compressed earth blocks (CEBs) as a function of kenaf fiber content, measured after 10 min according to the standard XP P 13-901 (XP P13-901, 2017). A significant increase in the absorption coefficient (CW10) was observed with higher fiber content. The fiber-reinforced CEBs with 1.5% fibers (CN20K1.5) exhibit the highest absorption capacity, with a value of 12.36 g/cm²·min½, compared to 9.98 g/cm²·min½ for those with 0.5% fibers (CN20K0.5). However, these results remain higher than those (8.40 g/cm²·min½) of alkali-activated CEBs without fibers (CN0K0). Despite these differences, all the tested CEBs (fiber-reinforced or not) showed low capillary absorption according to the standard XP P13-901 ($CW_{10} < 20$ g/cm²·min½).

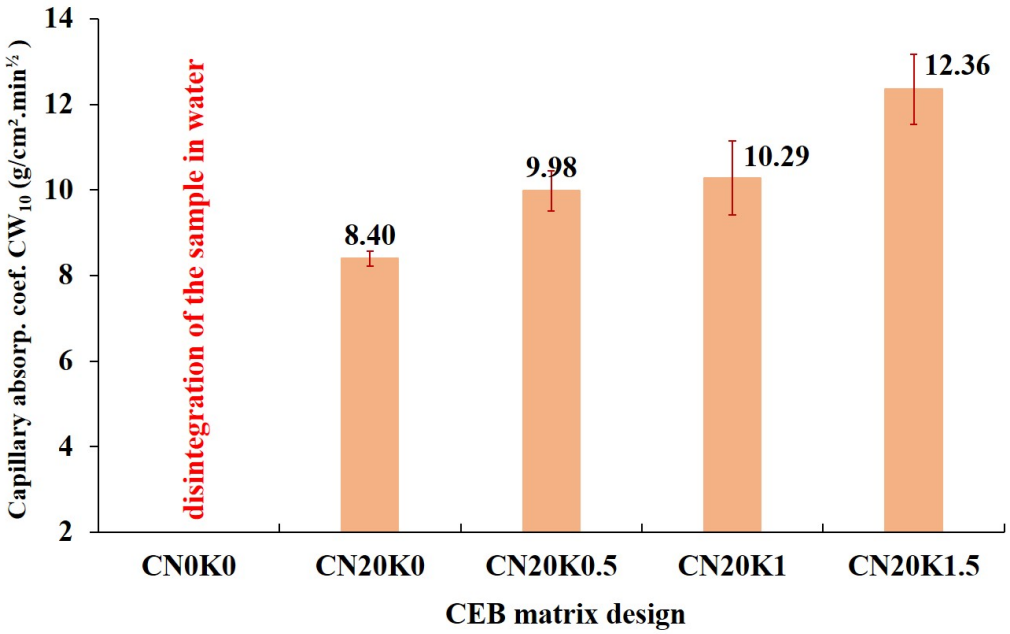

Figure 8. Capillary absorption coefficient of alkali-activated and kenaf-fibers-reinforced CEBs

Figure 9 illustrates the evolution of capillary absorption in CEBs as a function of time following the AFPC-AFREM protocol (AFPC-AFREM, 1997). This analysis confirms that absorption increases with fiber content, which is consistent with the results for water-accessible porosity (**Figure 6**) and ultrasonic pulse velocity propagation (**Figure 7**). Porosity, a key factor facilitating absorption, explains this increase in fiber content. The increase in the absorption coefficient was mainly attributed to the increased porosity induced by fiber incorporation (Taallah & Guettala, 2016). The hydrophilic nature of the fiber components (cellulose and hemicellulose) also promotes water absorption and retention (Sanou, Bamogo, et al., 2024). Similar observations have been reported by Labiad et al. (Labiad et al., 2022) for cement-stabilized, sisal fiber-reinforced CEBs, where capillary absorption also increased with fiber content.

3.2 Mechanical properties

3.2.1 Compressive strength

Figure 10 presents the dry and wet compressive strength results of the CEBs after 45 d of curing. The alkaline activation of CEBs at 20% led to a significant improvement in their mechanical strength, as evidenced by the increase from 0.31 MPa for unstabilized CEBs (CN0K0) to 4.26 MPa for

CN20K0-type CEBs. This value exceeds the minimum requirement of the XP P13-901 standard (XP P13-901, 2017) for earthen construction, demonstrating the effectiveness of alkaline activation in producing materials suitable for sustainable and high-performance construction. This enhancement in the mechanical properties can be attributed to the reaction of the alkaline solution with kaolinite present in laterite, resulting in the formation of geopolymer gels. These gels act as binders between particles, thereby increasing the compactness and cohesion of the samples (Belayali *et al.*, 2022; Idriss *et al.*, 2022; Sore *et al.*, 2025). Moreover, the high viscosity of the solution promoted better interparticle adhesion, further contributing to mechanical reinforcement. Similar observations were reported by Lemougna et al. (Lemougna *et al.*, 2014).

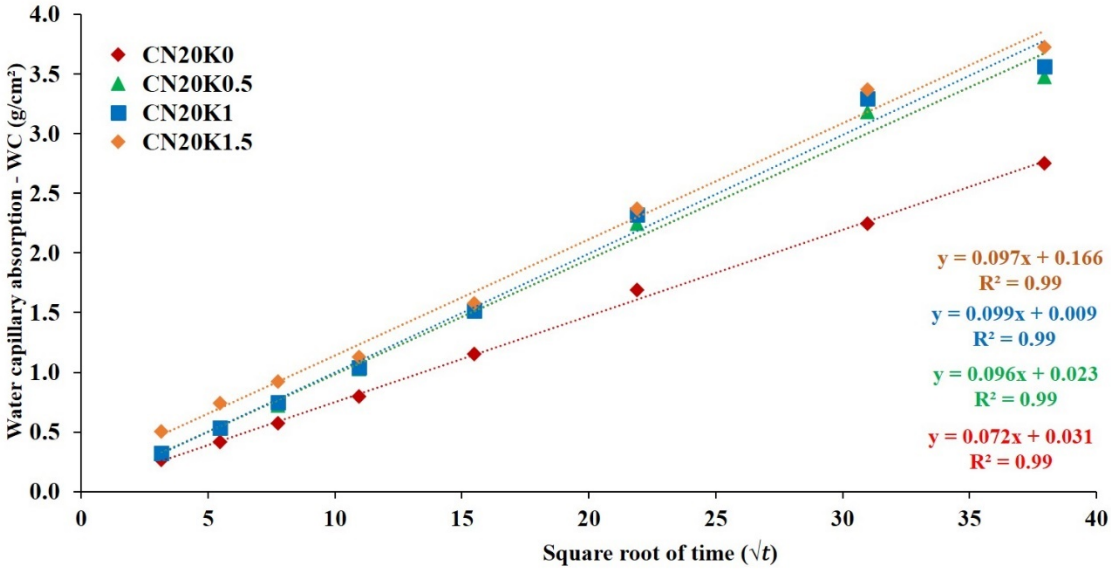

Figure 9. Capillary absorption of alkali-activated and kenaf-fibers-reinforced CEBs

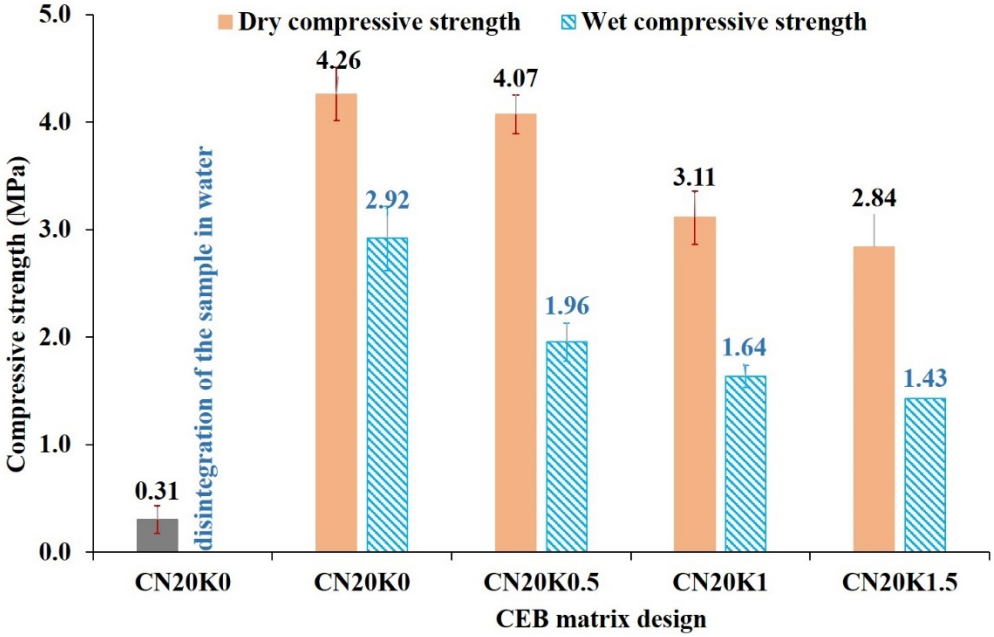

Figure 10. Compressive strength of alkali-activated and kenaf-fibres-reinforced CEBs

However, the addition of kenaf fibers to the alkali-activated CEBs matrix led to a decrease in the dry and wet compressive strengths. For fiber contents ranging from 0 to 1.5%, the dry compressive strength drops from 4.26 to 2.84 MPa (-33.3%), while the wet compressive strength falls from 2.92 to

1.43 MPa (-51%). Thus, it was observed that the wet strength accounted for approximately 50% of the dry strength. Despite this reduction, all dry compressive strength values of fiber-reinforced CEB remained above the minimum threshold of 2 MPa, as recommended by the XP P13-901 standard for earth partition wall construction. Several factors may explain this decline in mechanical properties, including the increased porosity resulting from fiber incorporation (**Figure 10**), which weakens the soil–fiber matrix adhesion (Lemougna *et al.,* 2014). A potential inhibitory effect between the alkaline solution and the fibers, or vice versa, and the hydrophilic nature of the fibers, which, at high concentrations (above 0.5% according to Kamwa et al. (Kamwa et al., 2025)), could delay water release during geopolymerization and curing reactions, thereby weakening the matrix cohesion. These findings are consistent with those of the previous studies. Taallah and Guettala (Taallah & Guettala, 2016) observed a similar decrease in lime-stabilized CEBs reinforced with date palm fibers. Zardari et al. (Zardari *et al.,* 2020) also reported a reduction in compressive strength with jute fibers. However, Sanou et al. (Sanou, Bamogo, *et al.,* 2024) noted an increase in the compressive strength of adobes up to an optimal kenaf fiber content of 0.2%, which was attributed to a more homogeneous microstructure where fibers filled pores and limited crack propagation. Beyond this threshold, excess fibers increased the porosity and weakened the matrix.

3.2.2 Flexural strength

Figure 11 presents the flexural strength results of non-stabilized, alkali-activated CEBs with and without kenaf fiber incorporation. Alkali activation induces a significant improvement in strength, increasing from 0.09 MPa (CN0K0) to 1.16 MPa (CN20K0). The addition of fibers further enhanced this property, with an optimal fiber content of 1%. The sample CN20K1 reaches a maximum strength of 1.49 MPa, representing a 28.4% increase compared to alkali-activated CEBs without fibers (CN20K0; 1.16 MPa). This optimal improvement at 1% fiber content can be primarily attributed to the high tensile strength of the fibers (802 MPa, **Table 3**) due to their cellulose content, as well as their homogeneous distribution within the matrix (Millogo *et al.,* 2014). The fibers act as reinforcement by absorbing stress after the rupture of the clay soil, thereby improving the material's ductility. However, beyond 1%, an excessive fiber content not only leads to localized concentration zones, limiting the mobilization of their tensile strength, but also increases the matrix porosity and reduces the flexural strength. These phenomena explain the decrease in flexural strength observed at 1.5% fiber content (CN20K1.5; 0.99 MPa). These results align with those of Sanou et al. (Sanou, Bamogo, *et al.,* 2024), who reported a similar improvement for cement- and kenaf fiber-stabilized adhesives at an optimal content of 0.2%. Additionally, Inga et al. (Inga *et al.,* 2023), observed a maximum flexural strength of 1.44 MPa for CEBs reinforced with 0.5% Agave americana fibers.

3.3 Thermal properties

Figure 12 presents the thermal properties of the different types of tested CEBs (unstabilized, alkali-activated, and fiber-reinforced) to evaluate their ability to improve the thermal comfort in housing. The studied parameters were thermal conductivity (λ) and thermal diffusivity (Dif). The results revealed an increase in these properties with the alkali activation of CEBs using 20% NaOH (CN20K0) compared to unstabilized CEBs (CN0K0). Thermal conductivity rises from 0.43 to 0.63 W/m·K, while thermal diffusivity increases from 0.22 to 0.30 mm²/s, representing relative increases of 46.5% and 36.4%, respectively. This improvement is attributed to the densification of the CEB matrix resulting from the addition of the alkaline solution, which triggers geopolymerization reactions and leads to the formation of a geopolymer gel. This gel coats the material particles, thereby enhancing

matrix cohesion and compactness (Sore, Nshimiyimana, Ouedraogo, *et al.,* 2025). Such compactness promotes an increase in the thermal conductivity and diffusivity.

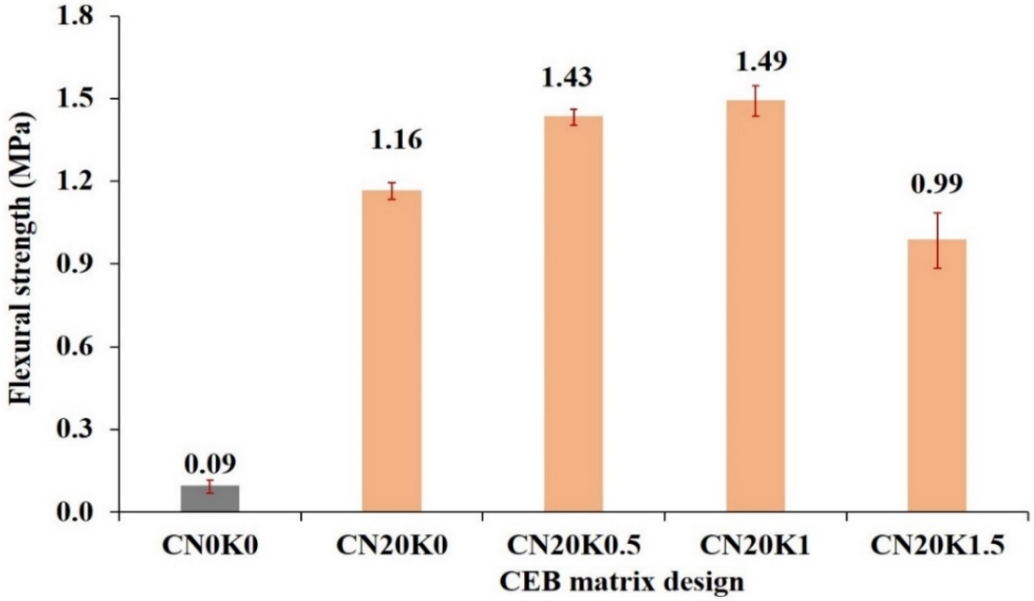

Figure 11. Flexural strength of alkali-activated and kenaf-fibers-reinforced CEBs

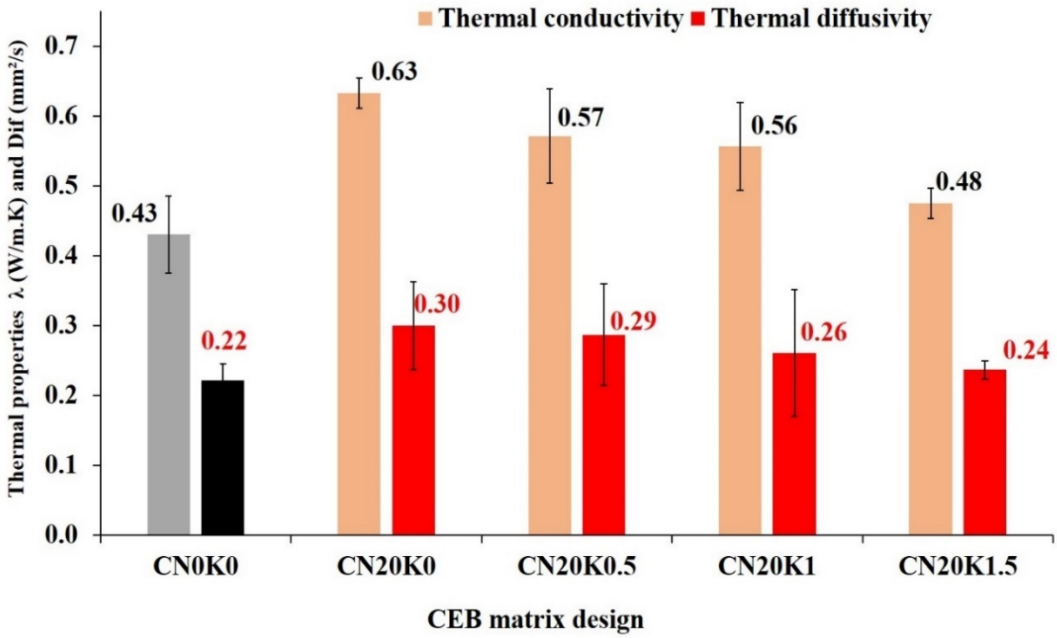

Figure 12. Thermal properties of alkali-activated and kenaf-fibers-reinforced CEBs

However, these two properties gradually decrease with the incorporation of fibers into alkali-activated CEBs. The CEBs containing 1.5% fibres (CN20K1.5) exhibit the lowest—and thus most favourable; values, with a thermal conductivity of 0.48 W/m·K and a thermal diffusivity of 0.24 mm²/s, compared to 0.63 W/m·K and 0.30 mm²/s for non-fibre-reinforced alkali-activated CEBs (CN20K0). This demonstrates that alkali-activated and fiber-reinforced CEBs offer better thermal performance than their non-fiber-reinforced counterparts. This improvement is attributed to the presence of cellulose in the kenaf fibers. Owing to its crystallinity, cellulose acts as a good thermal insulator (Kane *et al.,* 2024), thereby contributing to the reduction in the thermal properties of the composites.

Moreover, these findings align with the porosity measurements, which evolve inversely with thermal conductivity. The pores induced by the fibres trap air, whose low thermal conductivity (0.02 W/m·K) makes it an excellent insulator (Zoma *et al.,* 2020). Indeed, the presence of pores promotes air retention, and is recognized as one of the best insulating materials. These observations are consistent with those of Labiad et al. (Labiad *et al.,* 2022), who observed a decrease in the thermal conductivity of cement-stabilized CEBs with the addition of sisal fibers (0–0.5%).

3.4 Durability properties

3.4.1 Resistance to abrasion

Figure 13 illustrates the impact of alkaline activation and kenaf fibers on the abrasion resistance of Compressed Earth Blocks (CEBs). The addition of a 20% NaOH solution led to a significant improvement in this parameter. Indeed, the CN20K0 samples exhibited the highest abrasion resistance coefficient (18.44 cm²/g), far surpassing that of the CN0K0 samples (0.26 cm²/g). According to the XP P 13-901 standard, CN20K0-type CEBs can be classified in the CEB60 category, characterized by excellent abrasion resistance, while the less performing CN0K0 samples fall under the CEB20 category. This improvement in abrasion resistance through alkali activation is explained by the work of Sore et al. (Sore, Nshimiyimana, Ouedraogo, *et al.,* 2025), who identified three determining factors: high molarity of the activation solution, geopolymerization mechanisms, and solar curing. A high-molarity NaOH solution promoted the dissolution of aluminosilicates present in laterite, thereby triggering geopolymerization reactions. These reactions involve several stages, including the dissolution of aluminosilicate species, formation of oligomers, and their polycondensation into a geopolymeric gel. This gel coats the material particles, strengthening matrix cohesion.

Moreover, exposing the samples to a solar temperature of 40°C intensified these mechanisms by accelerating gel formation and stabilization of the gel. This results in a denser and more resilient matrix, which reduces the physical erosion caused by abrasion. This increased compactness minimizes particle loss, thereby enhancing the abrasion resistance of the CEBs. These observations are consistent with the findings of Palanisamy and Kumar (Palanisamy & Kumar, 2018), who demonstrated a positive correlation between the abrasion resistance, geopolymer content, and molarity of the activation solution. However, a decrease in the abrasion coefficient was observed alongside an increase in kenaf fiber content, a phenomenon similar to that observed for compressive strength. The alkali-activated CEBs with 0.5% fibres (CN20K0.5) exhibit the highest abrasion coefficient, reaching 15.98 cm²/g, compared to 11.12 cm²/g for those containing 1.5% fibres (CN20K1.5). Although these values remain lower than those of alkali-activated CEB without fibres (CN20K0, 18.44 cm²/g), they still exceed the reference value of 7 cm²/g set by the XP P 13-901 standard (XP P13-901, 2017), classifying them in the CEB60 category, resistant to abrasion, just like the CN20K0 samples.

Figure 14 highlights the condition of the CEB after the abrasion test, revealing significant degradation of the unstabilized sample (CN0K0). In contrast, the CN20K0 CEB appeared nearly intact with only a faint brush mark. However, the fiber-reinforced CEB showed more pronounced erosion traces on its surface, proportional to its fiber content, indicating progressive degradation due to fiber incorporation. This phenomenon can be explained by the poor adhesion between the fibers and the laterite matrix. Additionally, the increase in fiber content creates congestion zones with fiber–fiber interfaces that weaken the matrix, as demonstrated by Sanou et al. (Sanou, Bamogo, *et al.,* 2024) and Tallah and Guettala (Taallah & Guettala, 2016). The fibers located on the surface were easily pulled out by the test brush, increasing the degraded area. These findings align with those of Labiad et al.

(Labiad *et al.*, 2022), who also observed a decrease in the abrasion coefficient of cement-stabilized CEBs with the addition of sisal fibers.

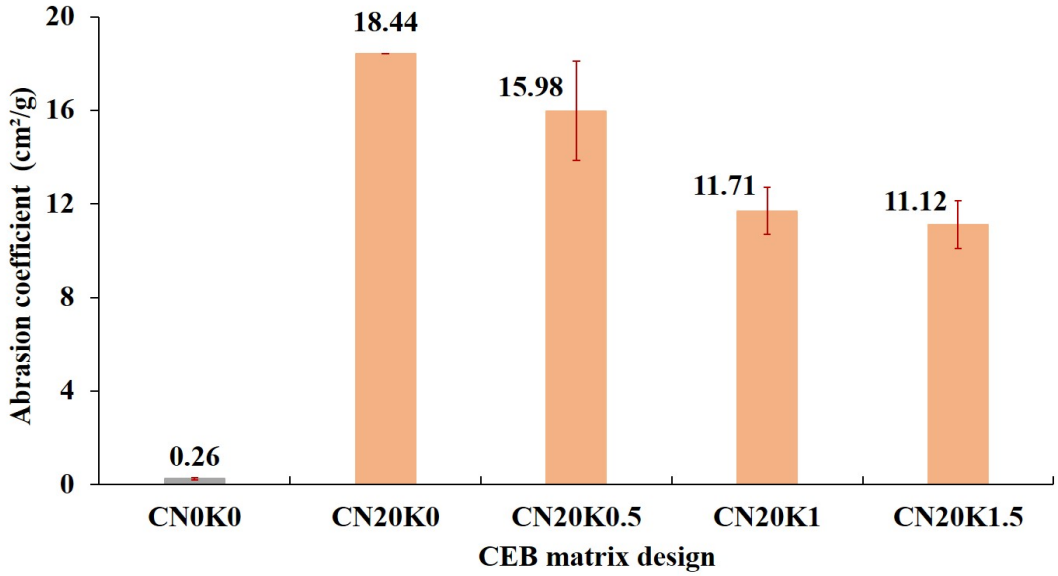

Figure 13. Abrasion resistance of alkali-activated and kenaf-fibres-reinforced CEBs

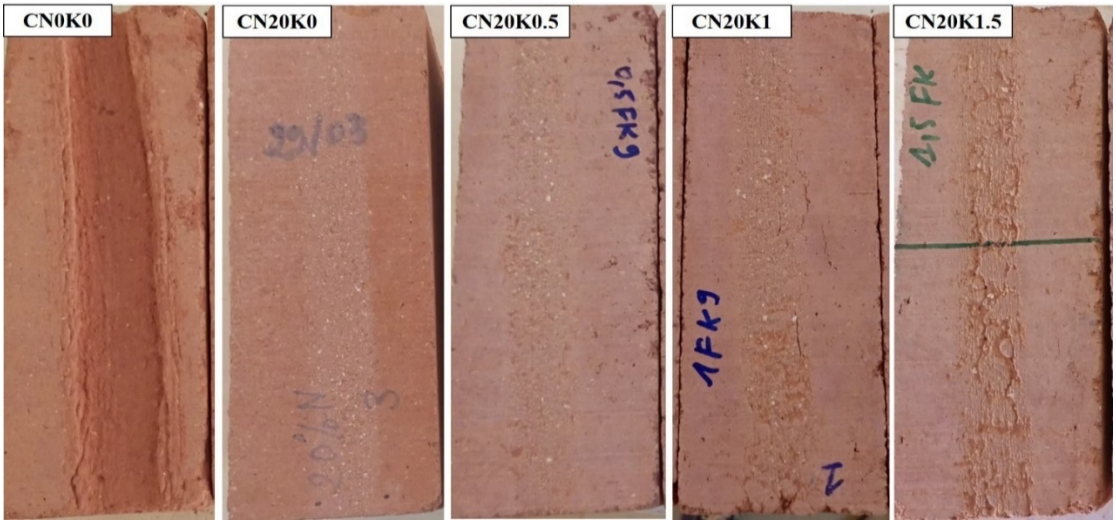

Figure 14. Appearance of CEBs after abrasion test

Figure 15 shows the correlation between the compressive strength and abrasion coefficient of alkali-activated and fiber-reinforced CEBs. This relationship reveals a logarithmic increase in the compressive strength with respect to the abrasion coefficient, indicating that a sample that is more resistant to physical erosion also exhibits better compressive strength. This correlation provides a predictive tool for estimating the compressive strength from abrasion test results, thereby avoiding the need for sophisticated and destructive testing methods, such as conventional compression tests. The high value of the coefficient of determination ($R^2 = 0.98$) confirmed the strong correlation between these two parameters, underscoring the reliability of this relationship.

3.4.2 Resistance to water erodibility

Figure 16 presents the results of the erodibility test for alkali-activated Compressed Earth Blocks (CEBs) as a function of the incorporated kenaf fiber content after applying water pressure for one hour. It was observed that the erosion depth and area increased proportionally with the fiber

content. The CEBs containing 1.5% fibers (CN20K1.5) exhibited the highest hydraulic erosion values, with 34.11% for the eroded area and 13.90 mm for the depth, compared with 9.20% and 7.13 mm for the CEBs with 0.5% fibers (CN20K0.5). These results remain systematically higher than those of alkali-activated CEBs without fibers (CN20K0), which show values of 0.86% for the area and 0.87 mm for the depth. According to the NZS 1998 standard (Allen *et al.*, 1998), all CEBs, whether fiber-reinforced or not, are classified as non-erodible, as their erosion depth remains below 120 mm/h.

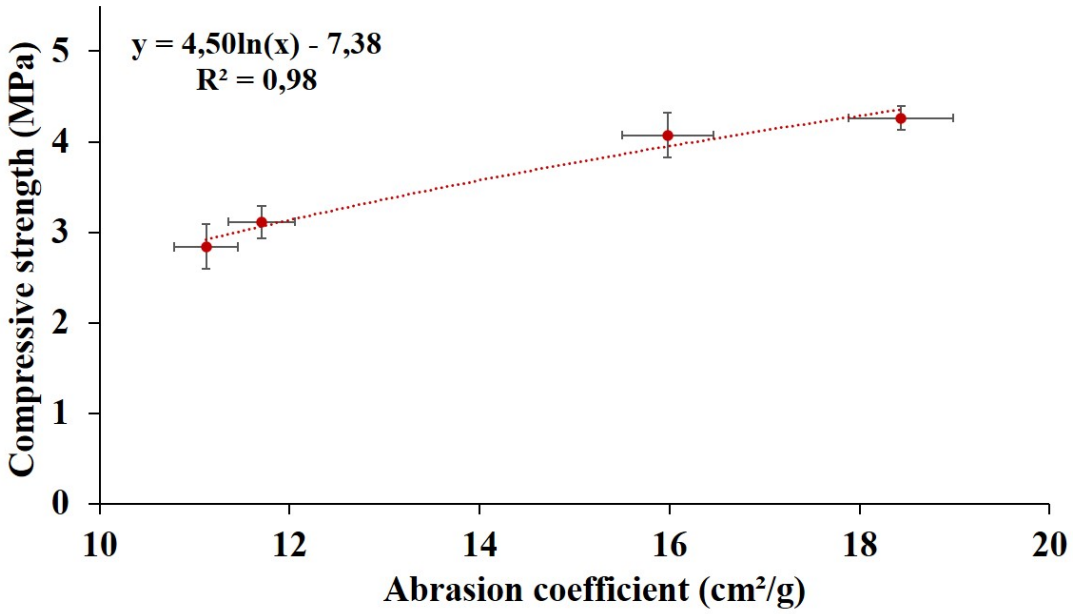

Figure 15. Correlation between compressive strength and abrasion resistance of alkali-activated and kenaf-fibers-reinforced CEBs

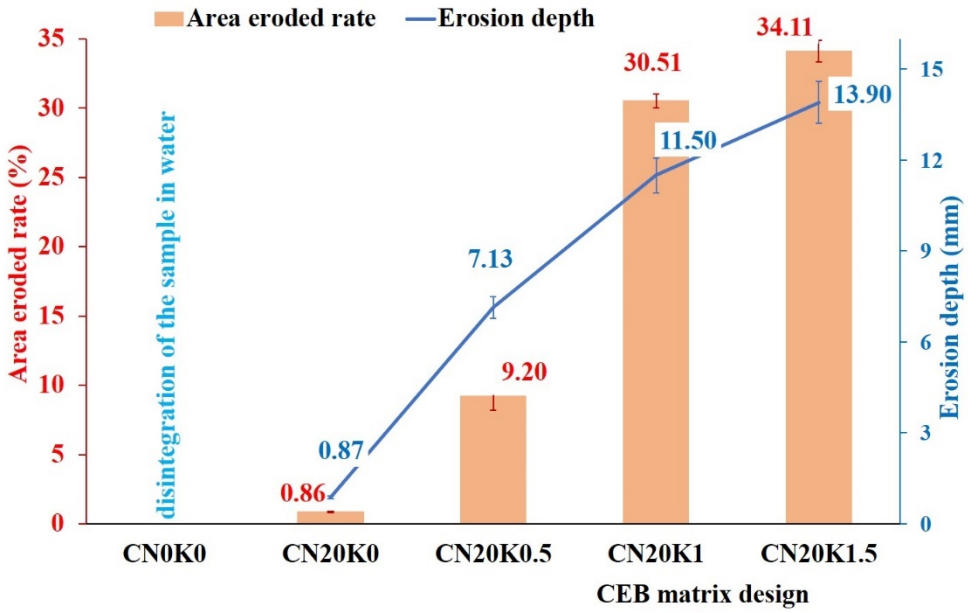

Figure 16. Resistance to water erodibility of alkali-activated and kenaf-fibers-reinforced CEBs

Figure 17 illustrates the appearance of the different types of CEBs after the erodibility test. Any traces of hydraulic erosion were barely visible on CN20K0, demonstrating its high resistance to water-induced damage. In contrast, the fiber-reinforced CEBs showed increasingly pronounced erosion marks with higher fiber contents. These marks were slightly visible on CN20K1 and were clearly more pronounced on CN20K1.5. This progression in erosion with increasing fiber content can be explained

by the increased porosity of the composites due to fiber replication zones (Taallah & Guettala, 2016). Under water pressure, the fibers detached more easily, creating cracks that promoted water penetration into deeper layers. This phenomenon generates increased internal pressures, resulting in greater erosion both at the surface and depth. Similar trends have been reported in studies by Obonyo et al. (Obonyo *et al.,* 2010), which showed an increase in erosion depth in cement-stabilized CEB s with the addition of coconut fibers.

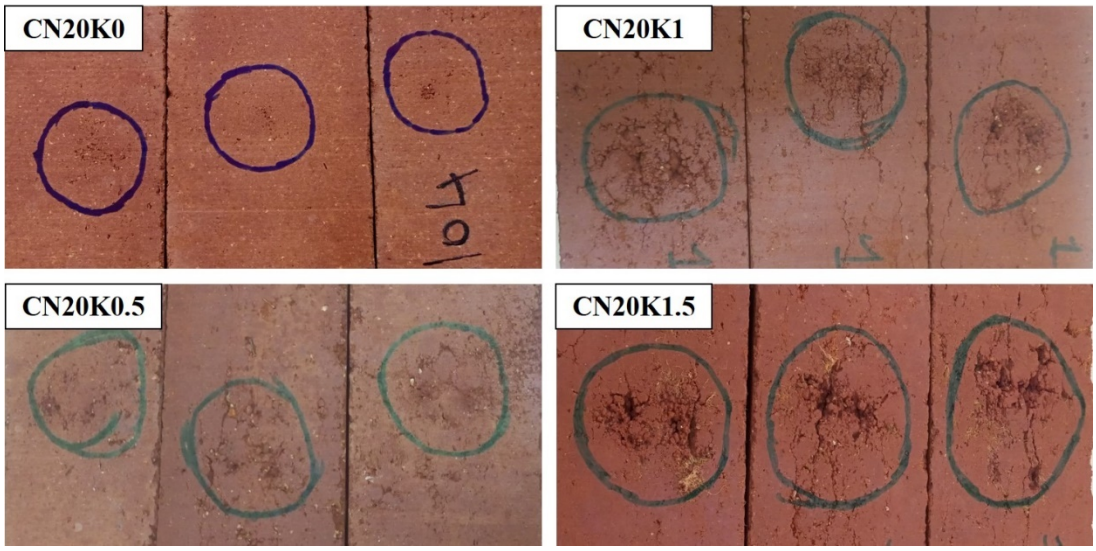

Figure 17. Appearance of CEBs after erodability test

Conclusion

The main objective of this study was to evaluate the influence of kenaf fibres on the engineering and durability properties of alkali-activated compressed earth blocks (CEBs) with 20% NaOH, compared to non-stabilised CEBs. The results revealed several significant trends.

- The addition of fibers led to a notable reduction in density, decreasing from 1659 kg/m³ (0% fibers) to 1591 kg/m³ (1.5% fibers), along with an increase in water-accessible porosity (from 34% to 37% for 1.5% fibers). This trend is explained by the partial replacement of high-density lateritic soil (2.88) with low-density kenaf fibers (1.05). The decrease in compactness was confirmed by the gradual reduction in ultrasonic pulse velocity, which decreased by 24.84% from 2001 m/s (0% fiber) to 1591 m/s (1.5% fiber). Additionally, the hydrophilic nature of the fibers contributed to the increased capillary absorption in the fiber-reinforced CEBs.
- In terms of mechanical properties, while alkali activation improved the dry compressive strength (4.26 MPa for CN20K0 vs. 0.31 MPa for CN0K0), fiber incorporation led to a decrease in this strength. Dry compressive strength dropped from 4.26 MPa to 2.84 MPa (-33.3%), and wet compressive strength decreased from 2.92 MPa to 1.43 MPa (-51%). Nevertheless, all values remained above the minimum threshold of 2 MPa, as recommended for CEB. In contrast, flexural strength improved by 28.4% compared to CN20K0, peaking at 1% fiber content (1.49 MPa for CN20K1).
- The thermal properties improved with fiber addition, showing a 23.8% reduction in thermal conductivity and a 20% decrease in thermal diffusivity at 1.5% fiber content (CN20K1.5) compared to alkali-activated CEBs without fibers (CN20K0). However, these performances were inferior to those of the non-stabilized CEBs (CN0K0).
- Regarding durability, abrasion and water erosion tests showed progressive decreases with increasing fiber content owing to insufficient adhesion between the fibers and the lateritic matrix.

Fiber-fiber interfaces also created weak zones, making fibers more susceptible to being pulled out under the effect of wire brushing or water erodability. However, all fiber-reinforced CEBs remained compliant and could be classified as abrasion-resistant or non-erodible.

This study highlights the significant impact of incorporating kenaf fibers into alkali-activated CEBs, altering their physical, mechanical, and thermal properties. The results demonstrate that these materials offer an interesting compromise between lightness, thermal performance, and strength, while meeting the minimum requirements for earthen construction. Among the tested formulations, CN20K1.5 CEB stands out as a viable solution for sustainable and eco-friendly housing construction despite a slight reduction in some intrinsic properties. Its adoption could not only enhance the performance of construction materials but also effectively valorize agricultural waste, contributing to a circular economy.

To further this research, several perspectives could be explored:

- Investigate the microstructure of fiber-reinforced alkali-activated CEBs to better understand the interfacial interactions between fibers, lateritic soil, and alkaline solution.
- Assess the long-term durability of fiber-reinforced CEBs, considering the potential degradation of organic (kenaf) fibers in the clay matrix under high alkalinity.
- Construct a prototype building to analyze the real-time behavior of fiber-reinforced CEBs (particularly CN20K1.5) and their thermal comfort performance.

Acknowledgement: The authors express their deep gratitude to *Pr. Aboubacar TOGUYENI*, coordinator of the partnership project between Nazi BONI University (UNB) and the World Food Programme (WFP) in Burkina Faso, for his invaluable support in the completion of this study. The authors also extend their sincere thanks to the management team of the 2iE Institute for facilitating the execution of a significant part of the research work in the LEMHaD laboratory. Finally, they wish to express their utmost appreciation to *Dr. S. Zara NIKIEMA*, Researcher at INERA Bobo, for kindly providing the kenaf fibers used in this study.

Disclosure statement: *Conflict of Interest:* The authors declare that they have no conflict of interest.

Compliance with Ethical Standards: This article does not contain any studies involving human or animal subjects.

References

AFNOR NF EN 933-1. (2012). Essais pour déterminer les caractéristiques géométriques des granulats - Partie 1 : détermination de la granularité - Analyse granulométrique par tamisage.

AFNOR NF EN 933-9. (2022). Essais pour déterminer les caractéristiques géométriques des granulats - Partie 9 : qualification des fines - Essais au bleu de méthylène.

AFNOR NF EN ISO 17892 -12/A1. (2021). Reconnaissance et essais géotechniques - Essais de laboratoire sur les sols - Partie 12 : détermination des limites de liquidité et de plasticité - Amendement 1.

AFNOR NF ISO 17892-4. (2018). Reconnaissance et essais géotechniques - Essais de laboratoire sur les sols - Partie 4 : Détermination de la distribution granulométrie des particules.

AFPC-AFREM. (1997). Détermination de la Masse Volumique Apparente et de la Porosité Accessible à l'Eau. Méthodes Recommandées pour la Mesure des Grandeurs Associées à la Durabilité. *Compte-Rendu Des Journées Techniques, Toulouse,* 121–124.

Ainane A., Taleb M., El-Hajjaji F., Hammouti B., Chetouani A., Ainane T. (2021), Study of dependence between two types of most abundant natural clays in Bejaad province (Central Morocco) using a statistical approach, *Mor. J. Chem.* 9(2), 210-220, https://doi.org/10.48317/IMIST.PRSM/morjchem-v9i2.22438

Allen, M., Hall, M., North, G., Gilkison, B., Morris, H., T., Drupsteen, North, G., Walker, R., & Christie, J. (1998). Materials and Workmanship for Earth Buildings. In NZS (New Zeal. Stand).

Belayali, F., Maherzi, W., Benzerzour, M., Abriak, N. E., & Senouci, A. (2022). Compressed Earth Blocks Using Sediments and Alkali-Activated Byproducts. *Sustainability (Switzerland)*, 14(6). https://doi.org/10.3390/su14063158

Bobet, O., Seynou, M., Zerbo, L., Bamogo, H., Sanou, I., & Sawadogo, M. (2020). Propriétés mécanique, hydrique et thermique de briques en terre crue amendées aux coques d'arachide. *J. Soc. Ouest-Afr. Chim*, 54–64. http://www.soachim.orgj.soc.ouest-afr.chim.

Bories, C., Aouba, L., Vedrenne, E., & Vilarem, G. (2015). Fired clay bricks using agricultural biomass wastes: Study and characterization. *Construction and Building Materials,* 91, 158–163. https://doi.org/10.1016/j.conbuildmat.2015.05.006

Dime, T., Sore, S. O., Nshimiyimana, P., Messan, A., & Courard, L. (2022). Comparative Study of the Reactivity of Clay Earth Materials for the Production of Compressed Earth Blocks in Ambient Conditions : Effect on Their Physico-Mechanical Performances. *Journal of Minerals and Materials Characterization and Engineering*, 10(01), 43–56. https://doi.org/10.4236/jmmce.2022.101004

Diop, M. B., Grutzeck, M. W., & Molez, L. (2011). Comparing the performances of bricks made with natural clay and clay activated by calcination and addition of sodium silicate. *Applied Clay Science*, 54(2), 172–178. https://doi.org/10.1016/j.clay.2011.08.005

Djibo, K.B., Sore S.O., Nshimiyimana P., Akodenyon D.Y., Messan A. (2024). Hydromechanical performances and durability of compressed earth blocks stabilised with metakaolin-based geopolymer binder. *Materials and Structures/Materiaux et Constructions,* 57(7), 169. https://doi.org/10.1617/s11527-024-02446-3

El Miz M., Loutou M., Aaddouz M., Tahani A., Mejdoubi E., Jodeh S., Azzaoui K. & Hammouti B. (2024) Thermal release of Thymol encapsulated into sodium, organic and pillared modified clay matrixes. *Chemical Papers,* 78, 1585–1599, https://doi.org/10.1007/s11696-023-03186-4

Ghavami, K., Toledo Filho, R. D., & Barbosa, N. P. (1999). Behaviour of composite soil reinforced with natural fibres. *Cement and Concrete Composites,* 21(1), 39–48. https://doi.org/10.1016/S0958-9465(98)00033-X

Ghyati S., Kassou S, El Jai M., El Kinani E.H., Benhamou M., Chang S.H. (2022). Thermal properties of clay containing polymeric reinforcement as an eco-friendly bio-insulation composite for buildings, *Journal of Thermal Analysis and Calorimetry,* 147, 7213–7228. https://doi.org/10.1007/s10973-021-11015-7

Giuffrida, G., Caponetto, R., & Cuomo, M. (2019). An overview on contemporary rammed earth buildings: Technological advances in production, construction and material characterization. *IOP Conference Series: Earth and Environmental Science,* 296(1). https://doi.org/10.1088/1755-1315/296/1/012018

Hamard, E., Cazacliu, B., Razakamanantsoa, A., & Morel, J. C. (2016). Cob, a vernacular earth construction process in the context of modern sustainable building. *Building and Environment*, 106, 103–119. https://doi.org/10.1016/j.buildenv.2016.06.009

Heller-Kallai, L., & Lapides, I. (2007). Reactions of kaolinites and metakaolinites with NaOH-comparison of different samples (Part 1). *Applied Clay Science,* 35(1–2), 99–107. https://doi.org/10.1016/j.clay.2006.06.006

Houben, H., & OA, D. O. (1998). Serie Tecnologies No. 11, Blocs De Terre Comprimée, Normes. Bruxelles: CRAterre-EAG ISBN, 2–906901.

Idriss, E., Tome, S., Rolande Aurelie, T. K., Nana, A., Nemaleu, J. G. D., Judicaël, C., Spieß, A., Fetzer, M. N. A., Janiak, C., & Etoh, M. A. (2022). Engineering and structural properties of compressed earth blocks (CEB) stabilized with a calcined clay-based alkali-activated binder. *Innovative Infrastructure Solutions,* 7(2), 1–9. https://doi.org/10.1007/s41062-022-00760-9

Inga, A. J. V., Zuñiga, J. G. B., Aburto, N. J. M., Solis, R. A. C., Tolentino, E. O. G., Espiritu, A. M. J., & Campomanes, G. P. (2023). Sustainable Blocks Reinforced with Agave americana L. Fiber and Its Mechanical Properties. *Civil Engineering and Architecture,* 11(4), 2072–2086. https://doi.org/10.13189/cea.2023.110428

Kagonbé, B. P., Guidana, M., Y, D. I. I., Loabé, P. A., Yaboki, E., Hamdja, N. A., & Alioum, P. S. (2023).

Environmental Implications of Artisanal Fired Brick Manufacture in Kaélé and Yagoua , Far North Region of Cameroon. *J. Mater. Environ. Sci,* 14(5), 548–559.

Kamwa, R. A. T., Mousi, J. B., Tome, S., Nemaleu, J. G. D., Gérard, M., Etoh, M. A., & Etame, J. (2025). Effect of treated palm fibers on the mechanical properties of compressed earth bricks stabilized by alkali-activated binder-based natural pozzolan. *International Journal of Ceramic Engineering and Science,* 7(1), 1–14. https://doi.org/10.1002/ces2.10246

Kane, M. N., Ndiaye, M., Touré, P. M., & Dione, A. (2024). Physical and Thermo-Mechanical Properties of Composite Materials Based on Raw Earth and Crushed Palm Leaf Fibers (Borassus aethiopum). *Materials Sciences and Applications*, 15(9), 358–377. https://doi.org/10.4236/msa.2024.159025

Komnitsas, K., Bartzas, G., Karmali, V., & Petrakis, E. (2021). Factors affecting alkali activation of laterite acid leaching residues. *Environments - MDPI,* 8(1), 1–21. https://doi.org/10.3390/environments8010004

Komnitsas, K., & Zaharaki, D. (2007). Geopolymerisation: A review and prospects for the minerals industry. *Minerals Engineering,* 20(14), 1261–1277. https://doi.org/10.1016/j.mineng.2007.07.011

Labiad, Y., Meddah, A., & Beddar, M. (2022). Physical and mechanical behavior of cement-stabilized compressed earth blocks reinforced by sisal fibers. *Materials Today: Proceedings,* 53, 139–143. https://doi.org/10.1016/j.matpr.2021.12.446

Labintan, C. A., Adadja, C. E., Gibigaye, M., Zahrouni, H., & Hattab, M. (2019). The Influence of Rice Straw on the Physical and Mechanical Properties of Banco, an Adobe Reinforced with Rice Straw. *International Journal of Engineering and Advanced Technology,* 9(2), 2363–2367. https://doi.org/10.35940/ijeat.a2242.129219

Latha, A. T., Murugesan, B., & Thomas, B. S. (2023). Compressed earth block reinforced with sisal fiber and stabilized with cement: Manual compaction procedure and influence of addition on mechanical properties. *Materials Today: Proceedings*. https://doi.org/10.1016/j.matpr.2023.04.373

Lemougna, P. N., Madi, A. B., Kamseu, E., Melo, U. C., Delplancke, M. P., & Rahier, H. (2014). Influence of the processing temperature on the compressive strength of Na activated lateritic soil for building applications. *Construction and Building Materials,* 65(2014), 60–66. https://doi.org/10.1016/j.conbuildmat.2014.04.100

Mastali, M., Shaad, K. M., Abdollahnejad, Z., Falah, M., Kinnunen, P., & Illikainen, M. (2020). Towards sustainable bricks made with fiber-reinforced alkali-activated desulfurization slag mortars incorporating carbonated basic oxygen furnace aggregates. *Construction and Building Materials,* 232, 117258. https://doi.org/10.1016/j.conbuildmat.2019.117258

Millogo, Y., Morel, J. C., Aubert, J. E., & Ghavami, K. (2014). Experimental analysis of Pressed Adobe Blocks reinforced with Hibiscus cannabinus fibers. *Construction and Building Materials,* 52, 71–78. https://doi.org/10.1016/j.conbuildmat.2013.10.094

NF P94-03. (2014). Sols : reconnaissance et essais - Détermination des références de compactage d'un matériau - Essai Proctor Normal - Essai Proctor modifié. AFNOR.

Nshimiyimana, P., Messan, A., & Courard, L. (2020). Physico-mechanical and hygro-thermal properties of compressed earth blocks stabilized with industrial and agro by-product binders. *Materials,* 13(17). https://doi.org/10.3390/ma13173769

Obonyo, E., Exelbirt J., Baskaran M. (2010). Durability of compressed earth bricks: Assessing erosion resistance using the modified spray testing. *Sustainability,* 2(12), 3639–3649. https://doi.org/10.3390/su2123639

Ongpeng, J., Gapuz, E., Andres, J. J. S., Prudencio, D., Cuadlisan, J., Tadina, M., Zacarias, A., Benauro, D., & Pabustan, A. (2020). Alkali-activated binder as stabilizer in compressed earth blocks. *IOP Conference Series: Materials Science and Engineering,* 849(1), 0–7. https://doi.org/10.1088/1757-899X/849/1/012042

Palanisamy, P., & Kumar, P. S. (2018). Effect of molarity in geo polymer earth brick reinforced with fibrous coir wastes using sandy soil and quarry dust as fine aggregate. (Case study). *Case Studies in Construction Materials*, 8(September 2017), 347–358. https://doi.org/10.1016/j.cscm.2018.01.009

Ramanandraibe, T. M., Rakotomamonjy, P., Robisonarison, G. J., & Andrianarison, E. R. (2023). Amélioration

Des Qualités Mécaniques D'une Brique De Terre Comprimée Stabilisée Au Ciment Par Trempe De Consolidation Au Silicate De Soude. *International Journal of Progressive Sciences and Technologies,* 38(1), 388. https://doi.org/10.52155/ijpsat.v38.1.5195

Sanou, I., Bamogo, H., Gnoumou, L. V. L., Dao, K., Ouedraogo, M., Saadi, L., Gomina, M., & Millogo, Y. (2024). Kenaf fibres from Burkina Faso valorization in the improvement of durability, thermal properties and fracture behavior of adobes amended with cement. *Industrial Crops and Products,* 219(June), 119077. https://doi.org/10.1016/j.indcrop.2024.119077

Sanou, I., Ouedraogo, M., Sore, S. O., Ouedraogo, R., & Millogo, Y. (2024). Hydric, Physical and Mechanical Behavior of Adobes Stabilized With Sugar Cane Molasses. *J. Mater. Environ. Sci, 15*(12), 1668–1683. http://www.jmaterenvironsci.com

Serebe, A. Y. A., Ouedraogo, M., Douani, A., Sanou, I., Estelle, W. J., Aubert, J., Gomina, M., & Millogo, Y. (2024). Optimization of kenaf fiber content for the improvement of the thermophysical and mechanical properties of adobes. *Construction and Building Materials,* 431(April), 136469. https://doi.org/10.1016/j.conbuildmat.2024.136469

Shinoj, S., Visvanathan, R., & Panigrahi, S. (2010). Towards industrial utilization of oil palm fibre: Physical and dielectric characterization of linear low density polyethylene composites and comparison with other fibre sources. *Biosystems Engineering,* 106(4), 378–388. https://doi.org/10.1016/j.biosystemseng.2010.04.008

Sore, S. O., Messan, A., Prud'homme, E., Escadeillas, G., & Tsobnang, F. (2018). Stabilization of compressed earth blocks (CEBs) by geopolymer binder based on local materials from Burkina Faso. *Construction and Building Materials,* 165, 333–345. https://doi.org/10.1016/j.conbuildmat.2018.01.051

Sore, S. O., Nshimiyimana, P., Messan, A., Prud'homme, E., Tsobnang, F., & Escadeillas, G. (2025). Chemical and Mineralogical Characterizations of Different Kaolinitic Clays from Burkina Faso: Feasibility for the Synthesis of Geopolymer Binders. *Geosciences,* 15(6), 230. https://doi.org/10.3390/geosciences15060230

Sore, S. O., Nshimiyimana, P., Ouedraogo, S., Banaou Djibo, K., Namoulniara, D. K., Semde, M., Sana, A., & Messan, A. (2025). Improvement of the performance of compressed earth blocks (CEBs) through alkali-activation of lateritic earth cured in the ambient sub-Saharan climate. *MRS Advances,* 0123456789, 6–10. https://doi.org/10.1557/s43580-025-01266-z

Taallah, B., & Guettala, A. (2016). The mechanical and physical properties of compressed earth block stabilized with lime and filled with untreated and alkali-treated date palm fibers. *Construction and Building Materials,* 104, 52–62. https://doi.org/10.1016/j.conbuildmat.2015.12.007

XP P13-901. (2017). Blocs de terre comprimée pour murs et cloisons Définitions- Spécifications - Méthodes d'essai - Conditions de réception. AFNOR, 37.

Zak, P., Ashour, T., Korjenic, A., Korjenic, S., & Wu, W. (2016). The influence of natural reinforcement fibers, gypsum and cement on compressive strength of earth bricks materials. *Construction and Building Materials*, 106, 179–188. https://doi.org/10.1016/j.conbuildmat.2015.12.031

Zardari, M. A., Lakho, N. A., & Amur, M. A. (2020). Structural behaviour of large size compressed earth blocks stabilized with jute fiber. *Journal of Engineering Research (Kuwait)*, 8(2), 60–72.

Zoma, F., Yonli, F. H., Malbila, E., Toguyeni, D. Y. K., & Hassel, I. B. (2020). Adding Hydrated Lime in a Material Made of Clayey Soil and Fibres: Formulation and Effects on Thermo-Mechanical Properties. *Journal of Minerals and Materials Characterization and Engineering,* 08(03), 149–161. https://doi.org/10.4236/jmmce.2020.83010